

Chapter 2

Evaluating Micro- and Macro-vascular Disease, the End Stage of Atherosclerosis, in Rat Models

James C. Russell

Abstract

Development of effective treatment or, more critically, preventative measures against atherosclerosis and cardiovascular disease will require animal models that mimic the disease processes seen in humans and permit identification of the genetic and physiological factors. The Rat is normally resistant to cardiovascular disease, but a number of genetic mutations make affected strains of rats highly susceptible to atherosclerosis and micro- and macro-vascular disease that is highly analogous to human disease. These models of obesity develop the metabolic syndrome and type 2 diabetes, hyperinsulinemia, hyperlipidemia, vascular and myocardial dysfunction, and end-stage lesions in the heart and kidney. The models offer the prospect of both genetic and molecular biology studies that are linked directly to spontaneous cardiovascular disease and exploration of putative preventative or treatment approaches, including pharmaceutical agents.

Use of small animal models of cardiovascular disease is dependent on appropriate experimental design and techniques that take account of the complex nature of the disease processes. Detailed experimental procedures for the use of rat models, including handling and treatment of animals, choice of experimental variables and endpoints, assay methods, and histological and electron microscopy techniques are covered in this chapter.

Key words: Atherosclerosis, rat, vascular function, vascular lesions, myocardial function, ischemic lesions, dyslipidemia, metabolic syndrome, histology, electron microscopy.

1. Introduction

Atherosclerosis has been recognized as an inflammatory process since the studies of Virchow and Rokitsky in the nineteenth century (1–3). It remains the major determinant of cardiovascular disease (CVD), the most important cause of death in developed societies and, increasingly, worldwide (4). CVD is not a single defined entity, but an end-stage pathophysiological state induced by a number of

poorly understood disease processes. CVD itself is a misnomer as it affects both micro- and macro-vascular vessels ranging from the aorta, major abdominal arteries, coronary, carotid, and intracerebral arteries to renal glomerular and retinal capillaries (5). The resultant, largely intimal, lesions lead to occlusion or rupture with ischemia, infarct (myocardial or other), or hemorrhage. At a micro-vascular level the results are glomerular sclerosis in the kidney, transient ischemic attacks in the brain, and retinal damage.

In recent years, a number of theories have been advanced to explain the development of atherosclerosis and CVD. The most prominent is based on the high lipid content of atherosclerotic lesions and the strong association between high-plasma low-density lipoprotein (LDL) cholesterol and CVD. This hypothesis has yielded extensive understanding of lipid and lipoprotein metabolism and the role of the genetic mutations that result in defects in the LDL receptor, familial hyperlipidemia, and premature CVD (6). While hypercholesterolemia is probably responsible for 35–40% of CVD, the 1995 forecast that imminent control of hypercholesterolemia would result in virtual elimination of CVD (7) proved to be premature. There is now a growing appreciation of the contribution (probably also in the range of 40%) of the pre-diabetic metabolic syndrome and type 2 diabetes to atherosclerosis and CVD (8). The metabolic syndrome is characterized by abdominal obesity, insulin resistance and hyperinsulinemia, and elevated plasma levels of the triglyceride-rich lipoprotein fractions VLDL (very low density lipoprotein) and chylomicrons. Both type 2 diabetes and metabolic syndrome are related to a strong environment–genome interaction, with some populations at particularly high risk (9). Population studies have begun to identify specific polymorphisms that play a strong role in the development of CVD (10), but are yet to define the mechanisms. These metabolic dysfunctional states are associated with striking micro-vascular damage contributing to a major fraction of renal disease, as well as myocardial and cerebral vascular disease. In addition to these factors, it has long been recognized that hypertension plays a role in exacerbating end-stage CVD.

Effective treatment protocols for atherosclerosis and CVD, and even more critically, prevention of the disease burden they impose, will require detailed understanding of the multiple contributing mechanisms. While human studies are essential to identify the issues, the mechanistic knowledge will have to come from studies in animal models. Such models must accurately mimic aspects of the human disease, and no one model can cover all dimensions of the multi-factorial origins of CVD. Relatively few animal models spontaneously develop CVD and many commonly used models depend upon highly abnormal conditions, for example, feeding high-cholesterol diets to species, such as the rabbit, that are herbivores (11). The critical issues involving the use of

animal models in the study of CVD have been reviewed recently (5). In summary, the best models are non-human primates, which are normally impractical for reasons of cost, longevity, and ethics, and swine, which again are relatively large and expensive, particularly the “mini pigs.” Effective small animal models are essentially confined to rodents, including rats, mice, and more exotic species such as hamsters and sand rats. Choice of an appropriate model is critical and dependent on the definition of the experimental question to be addressed. Use of an inappropriate model will vitiate the study. For instance, cholesterol-fed rabbits develop cholesterol-laden intimal lesions, but not if specific pathogen free; development of lesions is dependent on the chronic inflammatory state induced by bacterial pulmonary infections by agents such as *Pasteurella multocida* (12).

1.1. Selection of Animal Model

In balance, rats and mice are the optimal models for mechanistic studies of CVD, being small, relatively cheap, and amenable to genetic manipulation. None of the mouse models, including the various gene knockout strains, have been shown to spontaneously develop advanced atherosclerosis and CVD comparable to that seen in humans. These models generally require high-lipid diets or other environmental manipulation to induce vascular lesions and, thus, are best used to study the effects of hyperlipidemia (bearing in mind the significant differences in lipid metabolism compared to humans). Similarly, the genetically normal rat is highly resistant to atherosclerosis and requires both a high-cholesterol diet and treatment with thyrotoxic compounds to show significant hypercholesterolemia and vascular disease. However, there are a number of rat strains carrying mutations that lead to obesity, insulin resistance, hyperinsulinemia, and hypertriglyceridemia. One strain progresses to overt type 2 diabetes on a high-fat diet. These strains are suitable for study of early and full-blown diabetes and show both macro- and micro-vascular disease. The BB rat is a spontaneous model for type 1 diabetes, but has not been extensively studied for vascular disease. Streptozotocin has been widely used to induce pancreatic β -cell death and failure of pancreatic insulin secretion and, thus, a cytotoxin-produced quasi type 1 diabetes (13). This model is not really analogous to the autoimmunity-induced type 1 diabetes of the BB rat (14) and humans and may not accurately model vascular disease associated with type 1 diabetes.

1.2. The Fatty or *fa* Rat Strains

1. The Fatty Zucker

The *fa* rat mutation was initially described by Zucker and Zucker in 1961 (15) and consists of a glycine to proline substitution at position 269 of the leptin receptor (ObR), resulting in a 10-fold reduction in binding affinity for leptin (16). Rats homozygous for the *fa* mutation (*fa/fa*) develop a variant of the metabolic syndrome, becoming obese, moderately insulin resistant, and hypertriglyceridemic, but

with no progression to diabetes or cardiovascular complications (17). Heterozygous animals or those homozygous wild-type ($Fa/f\bar{a}$ or Fa/Fa) are lean and metabolically normal.

2. *The ZDF Rat*

Zucker Diabetic Fatty (ZDF) rats were developed from the original Zucker strain (18). When fed a high-fat chow, the $f\bar{a}/f\bar{a}$ ZDF rats, particularly the females, become insulin resistant and hyperinsulinemic and convert to a frank type 2 diabetes with very high plasma glucose levels as young adults. Diabetic ZDF rats exhibit many of the complications of the hyperglycemic diabetic state, particularly micro-vascular damage leading to glomerulosclerosis and retinopathy (19). In contrast, there are no reports of atherosclerosis or macro-vascular disease in these animals, although there is evidence of vascular dysfunction in aorta, coronary, and mesenteric arteries in adult to middle-aged obese ZDF rats, probably related to the overt diabetes (20). There is cardiac dysfunction that appears to be related only to hydronephrosis and not atherosclerosis (21).

1.3. *The Corpulent (cp) Strains*

In 1969, Koletsky isolated a mutation in a rat line originating in a cross between Sprague Dawley and SHR (spontaneously hypertensive) rats (22). The mutation, later designated *cp*, is a T2349A transversion, resulting in a Tyr763Stop nonsense codon leading to absence of the transmembrane portion of the ObR leptin receptor and, thus, of activity of all of the isoforms of the ObR (23). The original obese rats developed a fulminant atherosclerosis with advanced lesions, including dissecting aortic aneurisms (23). The original strain, now designated as SHROB, has been maintained for 60 plus generations in various laboratories. The atherosclerosis-prone character has been lost due to improper breeding and the strain is now commercially supported by Charles River Laboratories (Wilmington, MA). Over recent years, most of the *cp* rat strains have been established on a commercial basis, including those designated as: Crl:JCR(LA)-*Lep^r^{cp}*, SHHF/MccCrl*Lep^r^{cp}*, and SHR/OBKOLCrl-*Lep^r^{cp}* (details available at www.criver.com). See reference (5) for detailed background.

1. *The JCR:LA-cp Strain*

This strain has maintained the highly insulin-resistant and atherosclerosis-prone traits of the original Koletsky colony. Insulin resistance and hyperlipidemia develop rapidly in young male *cp/cp* rats of the JCR:LA-*cp* strain and are highly correlated with the development of CVD, both macro-vascular and micro-vascular (24–29). Most importantly, the *cp/cp* males spontaneously develop ischemic lesions of the heart (27) and are prone to stress-induced myocardial infarcts that can be fatal. Studies by scanning and transmission electron microscopy show extensive atherosclerotic lesions in major vessels throughout the arterial system of middle-aged *cp/cp* male rats (30). The lesions closely resemble the intimal atherosclerosis seen in human aorta and coronary arteries.

2. *The SHHF/Mcc-cp Strain*

The SHHF/Mcc-*cp* strain, developed from the SHR/N-*cp*, exhibits a cardiomyopathic/congestive heart failure trait, with a very high incidence of fatal congestive heart failure (31). This strain is a unique rat model of an important clinical problem and has been used to address issues related to cardiac dysfunction and ameliorative treatments (32, 33).

1.4. *Other Rat Strains*

Other rat strains that develop obesity and/or variations of type 2 diabetes have been described. These strains remain relatively poorly characterized and have not been demonstrated to develop atherosclerotic disease. The strains include the Goto-Kakizaki (GK) rat, a lean insulin-resistant strain (34); Zucker Diabetic Sprague Dawley (ZDSD), a strain with diet-sensitive development of hyperinsulinemic type 2 diabetes (*see* <http://www.preclinomics.com/>); the Otsuka Long-Evans Tokushima Fatty (OLETF) rat characterized by a mild type 2 diabetes and vascular dysfunction (35); and the SHR/NDmcr-*cp* rat, a strain derived from the original SHR/N-*cp* strain that exhibits hypertension, obesity, and vasculopathy (36).

1.5. *Experimental Endpoints*

Quantitative endpoints are an integral part of experimental design and allow detection and comparison of the severity of disease, as well as measurement of the efficacy of putative treatments. Choice of endpoint(s) is a function of the experimental aims. The principal CVD endpoints fall into metabolic, functional/physiological, and pathological categories. They are as follows:

1. *Metabolic Dysfunction*

Hyperlipidemias, the pre-diabetic state, and diabetes (type 1 and type 2) are the most important metabolic precursors to atherosclerosis, although there is significant overlap between these. While there are no established rat models of LDL receptor-mediated hypercholesterolemia, strains that develop obesity and/or the metabolic syndrome exhibit VLDL hyperlipidemia and chylomicronemia with delayed lipoprotein clearance (26, 37, 38). Measurement of fasting plasma lipids, especially of individual lipoprotein fractions, and postprandial kinetics provide indices of the pre-atherosclerotic status. Similarly, in strains that exhibit insulin resistance with hyperinsulinemia, fasting, and even more strongly postprandial, insulin levels are strongly correlated with vascular dysfunction and pathology.

2. *Vascular Function*

The earliest overt dysfunction in atherosclerotic disease is vasculopathy evident in hypercontractility responses to noradrenergic agonists and impaired endothelium-dependent relaxation. Classical isolated organ bath techniques, using rings of aorta or mesenteric resistance vessels, allow quantitative measures of vascular dysfunction in different kinds of arteries.

3. *Myocardial Function*

Isolated heart perfusion techniques allow direct assessment not only of myocardial function, but also of the coronary artery flow regulation and relaxation. Recent in vivo echo-cardiographic studies in rats have shown the possibility for chronic monitoring of impaired cardiac function in atherosclerosis-prone strains.

4. *Thrombosis*

Early atherosclerotic vascular dysfunction also leads to a prothrombotic status. This is characterized by platelet activation and impaired endothelial cell NO release, together with elevated plasma levels of plasminogen activator inhibitor-1 (PAI-1) and reduced lysis and persistence of intravascular thrombi. Changes in plasma PAI-1 and platelet function provide indices of vascular status.

5. *Renal Micro-vascular Dysfunction*

Glomerular capillaries are micro-arteries and prone to damage induced by hypertension and the underlying pathophysiological factors leading to atherosclerosis in larger vessels. The early-stage damage leads to increased glomerular permeability and leakage of albumin into the urine. Further development of the pathological processes leads to fibrosis and scarring, rendering the sclerosed glomeruli non-functional. The early stages can be quantified by the urinary albumin concentration and later stages by the measurement of glomerular filtration rate or by histopathological analysis of individual glomeruli.

6. *Vascular and Myocardial Lesions*

Atherosclerosis, as such, can be quantified in rat arteries, although this can only be done postmortem and in larger arteries. The lesions are relatively small, given the small size of the rat, and the most effective techniques are transmission electron microscopy (TEM) and scanning electron microscopy (SEM). TEM or light microscopy of thick sections from TEM specimens gives a cross-sectional view of a limited area of the arterial wall and allows identification of the internal composition of the lesion. In contrast, SEM gives a surface view of a large area of the intimal surface of the artery and reveals a range of lesions from raised lesions, to de-endothelialization, adherent thrombi, and luminal macrophage adherence and infiltration.

Myocardial lesions, the real end-stage of CVD, can be identified by light microscopy of conventional sections of the heart and quantified. Old, scarred, ischemic lesions constitute a preserved lifetime record of myocardial events that were large enough to be visible after the infarcted tissue had scarred and contracted.

7. *Micro-vascular Lesions – Glomerulosclerosis*

The fraction of the renal glomeruli that are sclerotic is a measure of accumulated micro-vascular damage in the rat. It is readily quantified by conventional histology of kidney sections.

2. Materials

2.1. Solutions

1. Krebs buffer (for aortic ring vascular function): 116 mM NaCl, 5.4 mM KCl, 1.2 mM CaCl₂, 2 mM MgCl₂, 1.2 mM Na₂PO₄, 10 mM glucose, and 19 mM NaHCO₃.
2. HEPES-buffered physiological saline: 142 mM NaCl, 4.7 mM KCl, 1.17 mM KH₂PO₄, 1.2 mM CaCl₂, 10 mM HEPES, 5 mM glucose.
3. Krebs–Henseleit solution (for heart perfusion and coronary artery function): 118 mM NaCl, 4.7 mM KCl, 1.2 mM CaCl₂, 2 mM MgCl₂, 1.2 mM Na₂HPO₄, 10 mM glucose, and 19 mM NaHCO₃.
4. 10% Neutral-buffered formalin (primary fixative for conventional histology, containing 3.7% formaldehyde): 37% formaldehyde solution diluted 1:10 with phosphate buffer, pH 7, also commercially available and ready to use.
5. Tyrode's solution (balanced salt solution to flush circulatory system prior to perfusion fixation): 137 mM NaCl, 12 mM NaHCO₃, 0.9 mM NaH₂PO₄, 4 mM KCl, 0.5 mM MgSO₄, 2.5 mM CaCl₂, and 5.0 mM glucose (pH 7.2).
6. Tyrode's solution with 2.5% glutaraldehyde (fixative solution for arterial system): basic balanced salt solution with addition of 2.5% EM grade glutaraldehyde.
7. Tyrode's solution with 1.25% glutaraldehyde and 1.85% formaldehyde (fixative for perfusion): fixation containing half effective concentrations of both EM and conventional fixatives, allowing subsequent further fixation for either EM light microscopy.
8. 4% Paraformaldehyde in 0.1 M sodium cacodylate (non-denaturing fixative allowing staining of fixed sections with specific antibodies): Polyoxymethylene 4% w/v in cacodylate buffer (*see* www.abdn.ac.uk/emunit/emunit/recipes.htm).
9. 1% Aqueous Osmium Tetroxide (OsO₄) (postfixative for TEM): *see* www.nrims.harvard.edu/protocols/Osmium_Tetroxide_Fix.pdf.
10. 2% Aqueous uranyl acetate (a heavy metal stain applied to increase contrast in TEM thin sections): *see* web.path.ox.ac.uk/~bioimaging/bitm/instructions_and_information/EM/neg_stain.pdf.

2.2. Equipment

1. Graz Vertical Tissue Bath System (Harvard Apparatus, Holliston, MA: www.harvardapparatus.com) or equivalent.
2. Isometric myograph system (Kent Scientific Corp., Torrington, CT: www.kentscientific.com/products).

3. Microliter syringe (Hamilton Company, Reno, Nevada: www.hamiltoncompany.com/syringes).
4. Isolated Heart Apparatus (size 3; Hugo Sachs Elektronik, March-Hugstetten, Germany), equipped with a Type 700 transit time flowmeter, *see* www.harvardapparatus.com.
5. Calibrated roller pump (i.e., Varioperpex II Pump 2120; LKB-Produkter, Bromma, Sweden, or equivalent).
6. Universal Servo Controlled Perfusion System (Harvard Apparatus, Holliston, MA: www.harvardapparatus.com).

2.3. Software

1. ALLFIT (a public domain program, *see* reference (42), program is available from this author or Dr. Peter J. Munson, e-mail: munson@mail.nih.gov).
2. Isoheart⁷W program V 1.2 (Hugo Sachs Elektronik, March-Hugstetten, Germany).
3. Photoshop (Adobe Systems Inc., San Jose, CA).

3. Methods

3.1. Animal Treatment and Handling

Due to the dependence of atherogenesis on a complex environment–genome interaction, the housing, diet, and handling of experimental animals must be carefully controlled. Stress, varying from that induced by shipping to the effects of unknown humans entering the animal room, can significantly alter metabolism and CVD progression. Any microbiological infection, from viruses to parasites such as pinworm, is contraindicated. Rats should be demonstrated virus antibody free (VAF) and monitored for parasites and virus antibodies on an ongoing basis. This may be arranged through commercial organizations such as Charles River Laboratories (www.criver.com/), Research Animal Diagnostic Laboratory, University of Missouri (www.radil.missouri.edu), or by the veterinary staff of the animal facility.

1. Diurnal Cycle

Rats are nocturnal and sleep during the light phase of the diurnal cycle. Thus, the animals' metabolism is reversed from that of humans and it is indicated that metabolic studies be conducted during the dark period of the diurnal cycle. Rats that are to be subjected to such studies are best maintained on a reversed light cycle, with lights off from 0600 to 1800 h, or equivalent timing adjusted for convenience in performing procedures. All manipulations of the rats are performed under a dim light in a dedicated procedure room.

2. *Housing*

Rats are traditionally maintained on aspen wood chip bedding in polycarbonate cages. However, we have converted our housing to a controlled isolated caging system (Techniplast, Slim Line™, Techniplast S.p.a., Buguggiate, Italy), in which all incoming and exhaust air is HEPA filtered. Our laboratory uses Lab Diet 5001 (PMI Nutrition International Inc., Brentwood, MO) as a standard food. The chow is available as pellets or as non-pelleted powder used for diets incorporating pharmaceutical or nutritional additives. The pelleted diet is also available in an autoclavable formulation which is important for maintaining animals in a secure barrier facility. Different diets are not interchangeable and are a significant variable that should never be changed during an experimental protocol.

Upon weaning, young rats are normally group housed for 1 week to reduce stress. Older rats are normally housed in pairs, as they are social animals and this can reduce stress levels. However, it is not good practice to house lean and obese male rats together beyond 6 weeks of age, as the lean rat will be aggressive toward the obese animal. Careful humidity control (50% relative humidity is indicated) is essential in the animal rooms. This is a significant problem in areas, such as Western Canada, where humidity levels can be very low, leading to ring tail disease in young animals.

Breeding colonies of genetic models are a core part of the research and should be carefully maintained. Staff must wear only facility clothing and footwear in the animal unit, as well as hats, masks, and gloves. Food and other items should be autoclaved before being brought into the unit and caging subjected to high temperature wash. These barrier precautions have been successful in preventing infection with viral or bacterial pathogens in genetic model colonies over many years. Because of the significant metabolic and physiological responses of rats to infectious processes, it is most important that experimental animals be maintained using similar protocols. Failure to do so will compromise the quality of the results.

3. *Breeding*

Breeding genetic models of a polygenetic disorder, such as atherosclerosis and CVD, requires a clear plan and allowance for inevitable genetic drift, which may result in the loss of some of the unique phenotypic characteristics of a colony. In the case of some strains with the *cp* gene, this has led to reduced severity of metabolic dysfunction. Most importantly, the inbreeding needed to create congenic strains also bred out the propensity for the development of the severe cardiovascular disease that is seen in the original Koletsky Obese SHR rat (22). To maintain the JCR:LA-*cp* rat, we ensured genetic stability of the colony through a formal assortive breeding program with ten separate lines, using a technique described by Pooley (39).

3.2. Drug Administration

In both mechanistic and pharmaceutical studies, there are often requirements to administer agents to rats in a defined manner, but with a caveat that the procedure should not be noticeable or stressful to the animals (*see Note 1*). Our standard approach is to incorporate agents (pharmaceutical or nutritional) in the rats' chow diet, measure food consumption, and control treatments on a per kilogram body weight basis. The method is as follows:

1. Agents to be incorporated, usually at doses in the range of 1–50 mg/kg BW/d, are intimately ground dry in a mortar and pestle with 5–10 g of powdered rat chow. The resultant powder is then mixed thoroughly with powdered chow to make a final mass of 1 or 2 kg in a small commercial pasta machine (Bottene, Marano, Italy (www.bottene.net)). For calculation of concentrations, based on rat body weights and food intake, *see Note 2*.
2. The mixed chow is moistened with approximately 200 mL of water, the volume being adjusted to give an appropriate consistency and extruded through a brass die machined to form 1 × 2 cm rounded pellets. The pellets of variable lengths are dried on a rack in a forced draft oven at 35°C.
3. Rats are weighed and food consumption determined twice weekly. New food is made up weekly based on the last week's food consumption data.

3.3. Anesthesia

Anesthesia is essential for surgical procedures and euthanasia, with blood and tissue sampling, while avoiding stress that will alter metabolic parameters (*see Note 3* for comments on appropriate and inappropriate methods). The method described is appropriate using either isoflurane or halothane. With either agent, the induction area and operating table should have an air scavenging system to ensure that personnel are not exposed to the anesthetic vapors.

1. Purge a bell jar chamber with isoflurane, 3.0–3.5% in oxygen at 1–1.5 L/min, delivered from a calibrated vaporizer.
2. Place rat in the chamber and continue isoflurane flow.
3. Once the rat loses consciousness (animal supine and non-responsive), transfer the rat to the operating/dissection area with heating pad and attach an anesthetic face mask over the nasal/mandible area. Maintain isoflurane flow at 200 mL/min and reduce concentration in increments to $2 \pm 0.5\%$ for maintenance.
4. Test depth of anesthesia (e.g. no eye movement on contact with sterile Q-tip, no pedal response to foot pinch, visual observation of breathing depth and rate). These should be monitored continually throughout the procedure.

5. *Euthanasia procedures* (see **Section 3.8**) may be initiated at this point.
6. *For recovery procedures*, apply a sterile lubricating ophthalmic ointment to eyes and shave the surgical area using electric clippers.
7. Apply povidone–iodine (Betadine 10%) solution with sterile gauze pads to surgical sites.
8. Wash the surgical sites with 100% ethanol using sterile gauze pads.
9. Place sterile surgical drapes around the surgical sites.

3.4. Blood Sampling

A method permitting repeated blood sampling is necessary in many studies and should be conducted on unrestrained animals to avoid stress. This also obviates the need for anesthesia, which can significantly affect the metabolic endpoints and lead to myocardial infarction in susceptible rats. The method described, sampling from a tail snip, depends upon calming the rat by quiet handling and minimal restraint.

1. The procedure should be conducted during the dark, active, part of the diurnal cycle in subdued light and in an isolated room free from noise and other activities. All personnel should be known to the rats and work quietly to avoid stress.
2. In either the animal or surgery room, a warming plate is prewarmed to $\sim 35^{\circ}\text{C}$ and should be warm to the touch, but not hot.
3. The rat is placed on the heating plate, covered with a wire basket for approximately 10 min to warm, and the tail to vasodilate.
4. The rat is gently removed from the heating plate, held on the forearm, and transferred to the procedure area. The rats tend to attempt to hide in the dark space under the upper arm and will remain quiet if handled gently.
5. The rat is held against the body of the operator by gentle pressure and the tail held in the fingers of the left hand. Using the other hand, the conical portion of the tail (0.5 mm tip) is removed with sharp sterile scissors, with care being taken not to cut the distal bone.
6. The tail is “milked” by gently stroking from the base to near the tip using the free hand and the blood drops that form on the tip are collected in a Microtainer[®] blood collection tube (BD Medical, Franklin Lakes, NJ) containing anticoagulant, as indicated.

7. When blood sample is complete, pressure is applied to the snipped tail with a sterile gauze pad until clotting occurs. The animal is then returned to its home cage to recover and is monitored.
8. The tail bleeding procedure may be repeated for up to five times in one day, with total volume not exceeding 15% of the blood volume of the rat ($\sim 75\text{--}80\text{ mL/kg}$ based on lean body mass (40)) or 2.5–3.0 mL for a 250–300-g rat). A recovery period of 1 week should be allowed before any additional blood sampling.
9. Rats are accustomed to the procedure 1 week in advance, through an initial sham procedure using a tail pinch with the fingers to simulate the tail cut.

3.5. Insulin/Glucose Metabolism

Insulin resistance, resultant hyperinsulinemia, and type 2 diabetes are major factors in CVD and need to be assessed quantitatively in many studies. A standardized meal tolerance test (MTT) procedure uses a tail bleed to obtain blood samples without restraint and with minimal disturbance (24).

1. The rat is deprived of food over the light period (normally overnight if animals are kept on a reversed light/dark cycle).
2. Two hours into the dark period, the initial (0 time) fasted blood sample is taken (*see Section 3.4*). A 0.8-mL blood sample is taken during each repeated sampling, and up to 1.5 mL can be collected in one sample without distress.
3. The rat is returned to its home cage and given a 5-g pellet of rat chow. The pellet is normally eaten within 15 min, and the timing is started when it is half consumed.
4. Further tail bleed samples are taken at intervals up to 150 min. Bleeding is stopped after each sample.
5. Samples are subsequently assayed for insulin and glucose.
6. Insulin-resistant rats maintain euglycemia under this protocol, but at the expense of a very large postprandial insulin response that can reach 1,000 mU/L (*see Note 4* for interpretation).

3.6. Plasma Lipid Measurements

There is an established practice in metabolic studies to measure plasma lipid concentrations in the fasted state (in the rat, after a 16-h period of food deprivation). This results in relatively consistent values, but does not reflect the metabolic status of an animal in its normal day-to-day situation. In contrast, measurements on blood samples taken 2–3 h into the light period, when the rat has eaten its first meal of the day, are more representative of the animal's ongoing metabolism (*see Note 5*).

3.7. Fat Challenge

Abnormal metabolism of apoB-containing, triglyceride-rich lipoproteins is a prominent component of the proatherogenic status accompanying the metabolic syndrome and type 2 diabetes. A fat challenge test allows quantitation of the dysfunction as an experimental endpoint, analogous to and conducted in a similar way to the insulin/glucose MMT.

1. Fat-supplemented food is pre-made using “English Double Devon Cream” (47% milk fat w/w). Mix 170 g of cream with 170 g of Lab Diet 5001 (PMI Nutrition International Inc., Brentwood, MO) powdered rat chow with gloved hands to form 5-g pellets (24% milk fat w/w).
2. Rats are fasted overnight as for MTT.
3. A fasted blood sample (0.4 mL) is taken 1 h into the dark period (0 time).
4. The rat is placed into its own cage with water ad libitum. A 5-g (pre-weighed) fat-enriched pellet is placed in the feed hopper.
5. When half of the pellet is eaten, the time is recorded as time 0, the reference point for the rest of the experiment.
6. Additional blood samples (0.4 mL each) are taken at time points 2, 4, 5, 6, 8, and 10 h.
7. Blood samples are collected in heparinized Microtainers.
8. Samples are spun in a centrifuge and plasma is pipetted into vials and stored at -80°C .
9. When all blood samples have been collected, the animal is returned to its normal feeding schedule.
10. Animals are allowed to return to their normal physiological state for 7 days before any other procedures or euthanasia is performed.

3.8. Euthanasia with Blood and Tissue Sampling

This technique enables fresh tissue samples to be taken, while providing an acceptable method of euthanasia.

1. Overnight fasting, prior to tissue collection, may be required depending on experimental endpoints.
2. Tissues and samples that may be taken include urine, plasma/serum, heart, aorta, kidney, liver, individual fat pads, and skeletal muscle and should be taken in this order. The tissues required should be clearly identified prior to the procedure and prepared for accordingly.
3. The rat is anesthetized as described in **Section 3.3** and placed in dorsal recumbency on the operating table.
4. The depth of anesthesia (surgical plane) is confirmed by the absence of pedal response, blink reflex, and breathing rate and depth. Breathing should be slower and deeper than normal.
5. If sterile samples are required, the incision site(s) should be shaved and prepared aseptically, using povidone-iodine and alcohol.

6. Using scissors, a 5–8-cm incision is made down the midline of the skin and then on the abdominal wall (linea alba) to expose the length of the peritoneal cavity.
7. If urine is required, it is collected first (from the bladder) with an 18G needle and syringe and placed in a tube on ice.
8. The chest is opened up the sternum using a substantial pair of scissors and the diaphragm cut to fully expose the heart. Cardiac puncture (left ventricle) is performed immediately with an 18G needle and 10-mL syringe. The blood is collected, placed in a heparinized tube, and stored on ice (*see* **Note 6**).
9. Rapid death of the animal is ensured by resection of the heart or cutting of the right atrium with resultant blood loss.
10. Remaining tissues or organs are removed, death confirmed, and the carcass bagged and labeled before disposal.

3.9. Aortic Vascular Function

Vascular contractile and relaxant dysfunction, both in resistance and conductance arterial vessels, is a major contributor to the pathological sequelae and a marker for atherosclerosis. Measurement of vascular function provides a quantitative index of vascular disease severity, based on isolated arterial segments.

1. Rats are euthanized as per **Section 3.8**.
2. After cardiac puncture and blood sampling, the heart is dissected and reflected forward allowing the aortic arch and thoracic aorta to be dissected and excised en bloc.
3. The heart and attached thoracic aorta are isolated, placed in ice-cold Krebs solution (*see* **Note 7**) in a Petri dish, and adhering fat and connective tissue trimmed off. This is done by slightly lifting the fat up and sliding the scissors, cutting away all extraneous tissue and fat while not hitting, nicking, or stretching the aorta.
4. The aorta is placed on a wet filter paper with clean buffer and kept moist. Using a sharp scalpel blade, slice into sections or rings no more than 3 mm long. Ensure that there is no “crushing” of the tubular tissue (this rubs the endothelial cells) by using a slight rolling motion. The paper and tissue rings are placed in a Petri dish with cold Krebs, carried to the apparatus, and the rings mounted within 10 min (*see* **Note 8**).
5. The aortic rings are mounted on stainless-steel hooks under a 1.5-g resting tension in 10 or 20-mL organ baths in a tissue bath system, bathed at 37°C in Krebs solution, and gassed with 95% O₂ and 5% CO₂.
6. The tissues are allowed to equilibrate for 45 min before measurements are started. During this time, the resting tension is readjusted to 1.5 g as required and the tissues washed every 15 min. Flushes and manual adjusting are kept to a minimum as they cause stress to the tissue.

7. Stock solutions (0.1 M) are made of the noradrenergic agonist phenylephrine (PE); the endothelium-dependent NO-releasing agent acetylcholine (ACh); the direct NO donor *S*-nitroso-*n*-acetyl-penicillamine (SNP); and the inhibitor of nitric oxide synthase, L-NAME (*see Note 9*).
8. PE solutions are added to the tissue baths with a microliter syringe (Hamilton Company, Reno, NV), cumulatively, to give concentrations of 10^{-9} – 10^{-4} M (*see Note 9*) and the contractile force produced measured and recorded as a concentration–response curve.
9. Rings are washed and equilibrated, then pre-contracted with PE to 80% of maximal contraction based on the dose–response curve.
10. The relaxant dose–response of the aortic rings to ACh and SNP is determined through cumulative additions of solutions to yield 10^{-9} – 10^{-4} M; normally half of the rings are treated with each agent.
11. L-NAME may be added to one or more baths at 10^{-4} M to inhibit NOS activity and to provide a direct measure of NO-mediated effects (41).

3.10. Mesenteric Resistance Artery Function

1. After euthanasia and removal of heart and/or aorta as above, the mesenteric arcade, 5–10 cm distal to the pylorus, is excised and placed immediately in ice-cold HEPES-buffered physiological saline.
2. Arterial rings (approximately 300 μ m in diameter) are cut to 2 mm lengths, threaded onto two stainless steel wires of 25 μ m in diameter, and mounted in an isometric myograph system (*see Note 10*).
3. Norepinephrine (NE) solutions are added to the tissue baths with a microliter syringe, cumulatively, to give concentrations of 10^{-8} – 10^{-5} M and the contractile force produced measured and recorded as a concentration–response curve.
4. Arteries are washed, equilibrated and pre-constricted to 50% of the maximal contractile response to NE, and cumulative concentrations of SNP (10^{-9} – 10^{-4} M) or ACh (10^{-9} – 10^{-6} M) are added. Reduction in the contractile force is recorded and expressed as % relaxation.

3.11. Interpretation of Vascular Function Data

Hypercontractile response to noradrenergic agonists, endogenous (such as NE) or synthetic (such as PE), is due to increased sensitivity of the vascular smooth muscle cells (VSMC) and leads to a propensity to vasospasm. Reduced relaxant response to SNP indicates that the VSMC have impaired sensitivity to NO and thus the hypercontractility originates in the medial layer of the arteries.

Reduced relaxant response to ACh indicates that the endothelial cells have reduced NO production and/or release and that the hypercontractility originates in the intima and endothelial cells.

The dose–response curves are best described by the Logistic Equation, with the four parameters being the minimum, or zero, response; the maximum response; the concentration of the agonist giving 50% of the maximum response (EC_{50}); and the slope of the curve at the EC_{50} . Changes in the parameters are important quantitative end points and need to be tested using appropriate statistical techniques. There are programs that calculate the parameters through curve fitting algorithms and plot both the raw data and best fit lines, for example, Prism (GraphPad Software Inc., La Jolla, CA). Statistical analysis based on the Prism-calculated values is not optimal and direct ANOVA using the raw data at individual agonist concentrations is misleading. The most powerful approach is the program ALLFIT (an open source program (42)) that treats the entire data sets as a whole, determines the best fit parameter values for each condition, and tests for significance of intergroup differences.

3.12. Heart Perfusion and Coronary Artery Function

The coronary arteries run intramurally (within the ventricular wall) in rats, making isolation of coronary arteries for myographic study difficult. However, cardiac vascular function can be studied effectively in the isolated perfused heart and yield data on coronary artery function.

1. Following the protocol in **Section 3.9**, the heart is excised rapidly, with ~1 cm length of the aorta intact, and placed in a Petri dish containing ice-cold Krebs–Henseleit solution (*see Note 11*).
2. The aortic root is cannulated using a polyethylene cannula, secured with fine cotton suture ligature, and mounted on an Isolated Heart Apparatus (*see Note 11*). The heart is perfused through the aortic root and coronary arteries at 37°C in the Langendorf (constant pressure) mode at 100 mmHg pressure with Krebs–Henseleit solution gassed with 95% O₂ and 5% CO₂.
3. Data are acquired using the Isoheart⁷W program V 1.2, including heart rate, perfusion pressure (maintained at 100 mmHg), coronary flow, LVP systolic, LVEDP, and dLVP/dt maxima and minima.
4. Reactive hyperemia is measured by stopping perfusate flow for 60 s. When perfusion is restored, there is a reactive increase in coronary artery flow. The peak postischemia flow is expressed as percent of the baseline flow.
5. Coronary endothelial and medial function is assessed by addition of bradykinin or SNP to the perfusate to give concentrations over the ranges of 10⁻⁹–10⁻⁵ M and 10⁻¹⁰–10⁻⁴ M, respectively (*see Note 11*). Dose–response curves are calculated and analyzed as described in **Section 3.11**.

6. Between perfusion studies the liquid handling system must be thoroughly flushed and cleaned overnight on a regular basis with a non-toxic detergent solution, as supplied by Hugo Sachs Elektronik, to prevent bacterial contamination.

3.13. Cardiac Histology

1. At euthanasia, the heart is rapidly excised without the aortic arch and placed in 10% neutral-buffered formalin solution (3.7% formaldehyde) for 4 h to fix.
2. The fixed heart tissue is cut transversely into four segments, base (aortic root) through to apex, using a sharp scalpel. The segments are placed into a tissue processing cassette, cut side up together in a standard array, and then dehydrated and embedded in paraffin using conventional techniques.
3. The paraffin blocks are sectioned and two adjacent sections stained with hematoxylin and eosin (H&E) and Masson's trichrome, respectively. The slides are examined blindly by an experienced observer and the incidence of the four stages of ischemic lesions recorded (*see Note 12*). Stages 1–3 are most readily visualized in the H&E stained slides, with the Masson's trichrome used to confirm Stage 4 (old, scarred) lesions. The number of lesions of each stage found in the individual hearts is averaged and statistical comparisons made using non-parametric statistical methods, such as the Rank Sum Test.

3.14. Renal Histology – Glomerulosclerosis

1. At euthanasia, one kidney is dissected and excised (always the same side, preferably left), cut using a sharp scalpel through the cortex to the pelvis on the long axis, and the two halves placed in neutral-buffered formalin to fix.
2. The fixed halves are placed in a tissue cassette, cut side up, dehydrated, and paraffin embedded using standard procedures. The blocs are sectioned and the sections stained with H&E or periodic acid-Schiff stain (PAS), which gives better definition, but is less commonly used.
3. Light microscopic images of four fields of view of each kidney are taken of the slides at $\times 2$ magnification using a digital camera system. The images are taken of the cortical area in a consistent pattern and with the operator blinded to the experimental group.
4. Images are visualized using Photoshop, examined blind, and all glomeruli in each field (minimum of 40 per kidney) rated as normal or sclerotic (*see Note 13*). Results are expressed as the percent of glomeruli that exhibit sclerosis.

3.15. Transmission Electron Microscopy

Electron microscopy is the definitive technique to detect and quantify atherosclerotic lesions in arteries of the size seen in the rat. The widely used alternatives, such as Oil Red O staining of the *en*

face preparation of the aorta, give no information on the nature of the lesions, only that lipid is present. Quantitative measurement of lesions also requires perfusion fixation as the artery contracts on loss of blood pressure. Common practice is to simply dissect the thoracic and abdominal aorta, which is pinned flat and stained with Oil Red O or Sudan Black. This protocol leads to variable changes in area and serious artifacts. There are two different electron microscopy techniques, transmission and scanning. Transmission electron microscopy (TEM) provides a cross-sectional view of the arterial wall at high magnification, permitting identification of the types of cells (macrophages, foam cells, fibroblasts, smooth muscle cells) and materials (lipid, proteoglycan, collagen) in the intimal space that underlies the endothelial layer. The integrity of the endothelial layer and intimal thickness can also be established.

1. Euthanasia is conducted as in **Section 3.8** up to Step 8, the stage of blood removal through the needle and syringe.
2. The syringe is removed leaving the 18G needle in place in the left ventricle. A cannula terminated in a male Luer-Loc fitting is attached to the needle in situ.
3. The right atrium is cut with a pair of fine scissors, reaching behind the heart on the operator's left, thus opening up a drainage site on the venous side of the circulation.
4. The cannula is perfused with Tyrode's solution at 100 mmHg pressure until ~100 mL has been passed using a fixed pressure device and continuous monitoring of pressure. The needle in the ventricle may shift against the ventricular wall and occlude, thereby reducing the flow rate, as can happen during blood sampling (*see Note 14*).
5. When the arterial system has been flushed, the perfusate is changed to Tyrode's solution containing 2.5% glutaraldehyde as fixative and the perfusion continued at 100 mmHg for a further 100 mL. If conventional histology is to be performed, this stage of the fixation procedure is conducted by perfusion with Tyrode's solution containing 1.25% glutaraldehyde and 1.85% formaldehyde (effectively half the concentration of glutaraldehyde for EM fixation and half the concentration of formaldehyde of the milder fixation for light microscopy). If immunochemical staining is to be used, the perfusion fixation is conducted with Tyrode's solution containing 4% paraformaldehyde in 0.1 M sodium cacodylate.
6. The fixed (stiff) internal organs are dissected out by cutting with fine scissors above the aortic arch and folding the block of tissue forward and out. The heart and aorta are dissected carefully with adherent fat and fibrous tissue. The aortic arch and/or thoracic/

abdominal segments are placed in 2.5% glutaraldehyde in Tyrode's solution and the heart in 10% neutral-buffered formalin. Both are fixed for several days, and the aorta will be kept indefinitely in the 2.5% glutaraldehyde solution.

7. The aortic arch is dissected free of all adherent fat and connective tissue using a dissecting microscope and micro-scissors. This is essential to prevent tissue damage resulting from excessive thickness and presence of water in the sample during processing.
8. The branches on the arch are cut short and the arch cut with fine scissors along the greater and lesser curves, yielding two curved mirror image halves of the arch. Samples (full thickness 1–2 mm in size) are cut from one half, focused on the lesser curve of the arch and the ostia of the branches.
9. Samples are postfixed in 1% aqueous OsO_4 for 1 h at 4°C and stained en bloc with 2% aqueous uranyl acetate for 1 h at room temperature. They are dehydrated through graded ethanol and embedded in Spurr's resin.
10. Toluidine blue-stained 1- μm sections from each block are mounted on glass slides for light microscopy. Ultrathin sections (50 nm) are cut on an ultramicrotome, mounted on hexagonal 200-mesh copper grids, and stained with uranyl acetate and lead citrate.
11. Toluidine blue-stained sections give a cross-sectional view of the intimal lesions and thickness can be quantified by image analysis. The ultrathin sections are examined in a transmission electron microscope and give information on cellular and subcellular elements of the lesions.

3.16. Scanning Electron Microscopy

Scanning electron microscopy (SEM) provides an image of the luminal surface at magnifications ranging from $\times 10$ to $\times 10,000$. The entire surface of a sample, such as the whole aortic arch, can be examined for the presence of endothelial damage, raised intimal lesions, adherent macrophages, and thrombi (at both large and cellular scales). Images can be recorded at a resolution of 4,000+ lines and quantified.

1. Follow Steps 1–7 from **Section 3.15**.
2. The aortic arch halves used for SEM are postfixed in 1% aqueous OsO_4 for 1 h at 4°C, dehydrated through graded ethanol, critical point-dried from propylene oxide in a critical point dryer, mounted on aluminum stubs, and sputter coated with gold.
3. The samples are examined overall in a scanning electron microscope, at magnifications ranging from $\times 4$ to $\times 4,000$. Particular attention is paid to the lesser curve of the arch and the regions adjacent to the ostia of the branches, which are atherosclerosis prone.

4. All lesions are recorded as a digital image at 4,000 lines resolution and each type of lesion is assigned a severity score, based on areal extent and character of the lesion, for each animal (*see* **Note 15**).

4. Notes

1. We have established that obese or metabolically abnormal rats are hyperresponsive to the stress of physical restraint and simple handling with significant and long-lasting metabolic changes (43, 44). These changes can seriously compromise experimental data. For example, a common approach to administration of agents to rats has been to inject the agent on a daily basis (subcutaneously, intramuscularly, intraperitoneally, or through the tail vein). All routes involve repeated restraint and some pain and are thus stressful. The technique of gastric gavage similarly imposes a repetitive stress and additionally creates a necessity to dissolve or suspend the agent in an aqueous medium, which can often be difficult.
2. The concentration of food additives may be calculated as follows:

$$C(\text{mg/kg}) = BW(\text{kg}) \times D(\text{mg/kg}) / FC(\text{g/d})$$

where C is the final concentration of additive in the prepared food, BW is the body weight determined $2 \times$ per week, D is the desired dose/day, and FC is the measured daily food intake of the group of animals. This procedure has been demonstrated to give dosages within $\pm 3\%$ of calculated values (45).

3. Rats have conventionally been anesthetized with pentobarbital which is injected intraperitoneally. More recently, other agents, such as ketamine and xylazine, have been used (46). Obese and metabolically dysfunction rat strains, in particular, do not tolerate these injectable agents well. Typically rats with large fat depots do not reach a surgical plane of anesthesia using a normal dosage and a further increment must be given. Following this, the anesthesia becomes too deep and irreversible respiratory depression develops with rapid death.
4. The conventional method of assessing insulin and glucose metabolism in the rat has been the intravenous glucose tolerance test (IVGTT), with the euglycemic insulin clamp being the ultimate approach. Both methods present serious problems in obese insulin-resistant rats. Because the IVGTT shows relatively small differences in the rate of clearance of an injected glucose load (typically 0.5 g/kg) as a function of insulin sensitivity/resistance (47), it is difficult to detect experimental changes in the severity

of insulin resistance using this test. A euglycemic insulin clamp can give detailed information on the glucose clearance and hepatic output, effectively as a concentration response curve against plasma insulin, and is practical in obese rats (48). However, the procedure is complex, lengthy, and requires either that the rat be anesthetized throughout or that indwelling cannulae be surgically implanted in advance. The relatively lengthy anesthesia required for both the IVGTT and the euglycemic insulin clamp leads to very significant stress in these rats. Obese rats respond to stress with significant variations in insulin and glucose metabolism, as well as central nervous system changes (43, 44), all of which can obscure experimental effects.

In contrast to the IVGTT, which bypasses the complex gut hormone responses to food intake, a meal tolerance test (MTT) is much more sensitive to changes in insulin and glucose metabolism. The standardized MTT does not require anesthesia, minimizes stress on the rats, and can be administered repeatedly to the same animal (24). The insulin response is short-lived and the plasma concentrations at 30 min provide an excellent index of insulin sensitivity, which is essentially the plasma insulin level required to maintain euglycemia. Treatments that lower insulin resistance result in a reduced 30 min insulin concentration and can, in some cases, completely prevent the postprandial insulin response (45, 49).

5. Fasting plasma triglyceride and insulin levels are significantly higher in obese insulin-resistant rats and are higher again in the fed state, but glucose concentrations are in the normal range. The development of hyperinsulinemia and hypertriglyceridemia as the juvenile rat matures can be followed sensitively in the fed state (50), but is obscured in the fasted state.
6. Cardiac puncture requires access via the diaphragm, which in turn collapses the lungs, and initiates hypoxia, painless, irreversible unconsciousness, and death. It should be kept in mind that once the chest is opened, no further anesthetic agent reaches the circulation and that the brain levels will drop rapidly due to uptake by fatty tissues. Thus, it is essential that the cardiac puncture and blood sampling be initiated immediately before the level of anesthesia falls.

A volume of 8–11 mL of blood is readily collected. Good collection depends on the needle puncture of the ventricle being made about $\frac{1}{3}$ of the way up the heart from the apex at an angle of about 30° and the bevel of the needle facing up. If the blood does not flow readily from the beating heart, the bevel of the needle is obstructed against the ventricular wall and the angle of the needle should be reduced with gentle pressure applied toward the back of the heart.

7. Krebs buffer solution for aortic ring vascular function is made from two stock solutions that are made up in RO water at $10\times$ and $20\times$ final concentrations, aliquoted into 200-mL screw-capped tubes, and stored at -20°C .

Solution 1 g/L		Solution 2 g/L	
NaCl	6.87	NaHCO ₃	2.09
KCl	0.35	Glucose	1.81
MgSO ₄	0.24	Na ₂ HPO ₄	0.131
CaCl ₂	0.176		

1. Keep the two solutions separate to prevent precipitation.
 2. Prepare Krebs by mixing 200 mL of solution 1 and 200 mL of solution 2 into 2 L of RO water.
 3. Check pH after solution has been bubbled for $\frac{1}{2}$ h with 95% oxygen/5% CO₂ in the baths at 37°C to saturate. It may be necessary to adjust pH to ~ 7.4 with 0.1 M HCl.
 4. 0.1 M HCl can be made by adding 8.6 mL of concentrated HCl to 1 L of RO water. (Will usually need to add ~ 17 mL to 1 L of Krebs to bring pH down.)
8. Aortic tissue is sensitive and must be harvested immediately after exsanguination, with care not to injure the endothelial layer. When all external fat and clotted blood from inside aorta are removed, place the aorta on a wet filter paper with clean buffer and keep moist. Using a sharp scalpel blade, slice into sections no more than 3 mm long. Carefully ensure that there is no “crushing” of the tubular tissue (this rubs the endothelial cells) using a slight rolling motion. Damaged endothelial cells will not secrete NO, either spontaneously/physiologically or in response to ACh, leading to an absence of NO-mediated relaxation and hypercontractility.
9. Protocol for preparation of agonist/antagonist solutions.

Agent	Mol weight	g/mL	Stock M	Further dilutions
PE	203.7	0.0204 g	10^{-1} (10^{-4} in bath)	*
ACh	181.7	0.01817	10^{-1} (10^{-4} in bath)	*

(continued)

Agent	Mol weight	g/mL	Stock M	Further dilutions
L-NAME	269.7	0.02697	10^{-1} (10^{-4} in bath)	No further
SNP	222	0.0222 §	10^{-1} (10^{-4} in bath)	§

- Use RO water for all solutions.
- Baths – 10 mL; * – 0.1 mL of stock conc in 1 mL RO water = 10^{-2} (or 10^{-5} in bath); 10^{-6} mol/L would be made with 0.1 mL of 10^{-5} mol/L made up to 1 mL with RO water and so forth.
- § – Will not dissolve in 1 mL, use 10 mL (10^{-5} mol/L in bath will give full effect).
- SNP – *S*-nitroso-*n*-acetyl-penicillamine; ACh – acetylcholine chloride.
- L-NAME – *N*-nitro-*L*-arginine methyl ester; PE – phenylephrine hydrochloride.

All equipment must be cleaned daily to prevent buildup of salts and bacterial contamination.

10. Mesenteric arteries of 300 μ m diameter are resistance arteries, in contrast to the aorta, which is a conductance artery. These different vessels have different physiological responses and give results that provide a range of information on vascular dysfunction. The agonists and equipment used are different to suit the type of artery being studied.
11. Rat hearts are perfused on an Isolated Heart Apparatus (size 3) (Hugo Sachs Elektronik, March-Hugstetten, Germany), equipped with a Type 700 transit time flowmeter, and data acquisition with the Isoheart^{7W} program V 1.2 (Hugo Sachs). Perfusion is performed using Krebs–Henseleit solution gassed with 95% O₂ and 5% CO₂. Bradykinin (a non-cholinergic, endothelium-dependent vasodilator acting on its own BK receptor) and SNP (a direct NO donor and vasodilator) are added to the perfusate through a “T” fitting upstream to the debubbling chamber using a calibrated roller pump. The following variables are measured; heart rate, perfusion pressure (maintained at 100 mmHg), coronary flow, LVP systolic, LVEDP, and dLVP/dt maxima and minima. Reactive hyperemia is measured following 60 s of stopped perfusion, with the peak postischemia flow expressed as percent of the baseline flow. ACh is not used to assess endothelial cell function, as the coronary artery does not express cholinergic receptors, but does have BK receptors.

12. The myocardial lesions are a record of end stage of CVD, over the life time of the rat. They are identified as follows:

Stage 1: areas of necrosis. These are recently infarcted areas of an age from ~6 to 24 h, before chronic inflammatory cell (CIC) infiltration has been established, and characterized by a darkened “glassy” appearance in the histologic section.

Stage 2: areas of cell lysis with CIC infiltration. These are lesions aged 24 h to 3 week. The most recent lesions show only numerous chronic inflammatory cells infiltrating the necrotic zone, evident by dark prominent staining of the nuclei. Advanced Stage 2 lesions are characterized by cell “drop out” (empty or unstained areas where myocytes have been lysed and scavenged by the CIC).

Stage 3: nodules of chronic inflammatory cell infiltration. These are small isolated nodules of CIC without evidence of lysis of myocytes, appear in normal rats, and are probably not significant.

Stage 4: old, scarred lesions. Stage 4 lesions are the most important, as they reflect the cumulative record of earlier stage lesions that were large enough to remain identifiable after the scarring and contraction of the repair process.

Micrographs of typical myocardial lesions are shown in **Fig. 2.1**. The mean incidence of each stage yields a consistent index of the ischemic damage to the myocardium (51).

13. Characterization of glomeruli as sclerotic has been summarized, with excellent representative micrographs (52). Sclerotic glomeruli show enlarged Bowman’s space, often fissures in the glomerular tuft and fibrosis. The use of Photoshop, with high resolution recorded microscopic images, allows both large-scale, low-magnification assessment and higher magnification (electronically) examination of individual glomeruli.
14. Good perfusion fixation is dependent on maintaining the desired 100 mmHg pressure in the ventricle. If the needle occludes, partially or completely, flow will drop and pressure upstream from the heart at the pressure transducer will rise, due to the normal drop in pressure within the length of tubing leading to the heart. The needle should be gently moved away from the ventricular wall by trial and error until the measured pressure drops slightly and the flow resumes. The flow can also be monitored through the outflow from the cut right atrium. An effective fixation is usually accompanied by sudden and widespread muscle spasm throughout the body. Perfusion should be continued until the entire 100 mL of fluid has been infused.

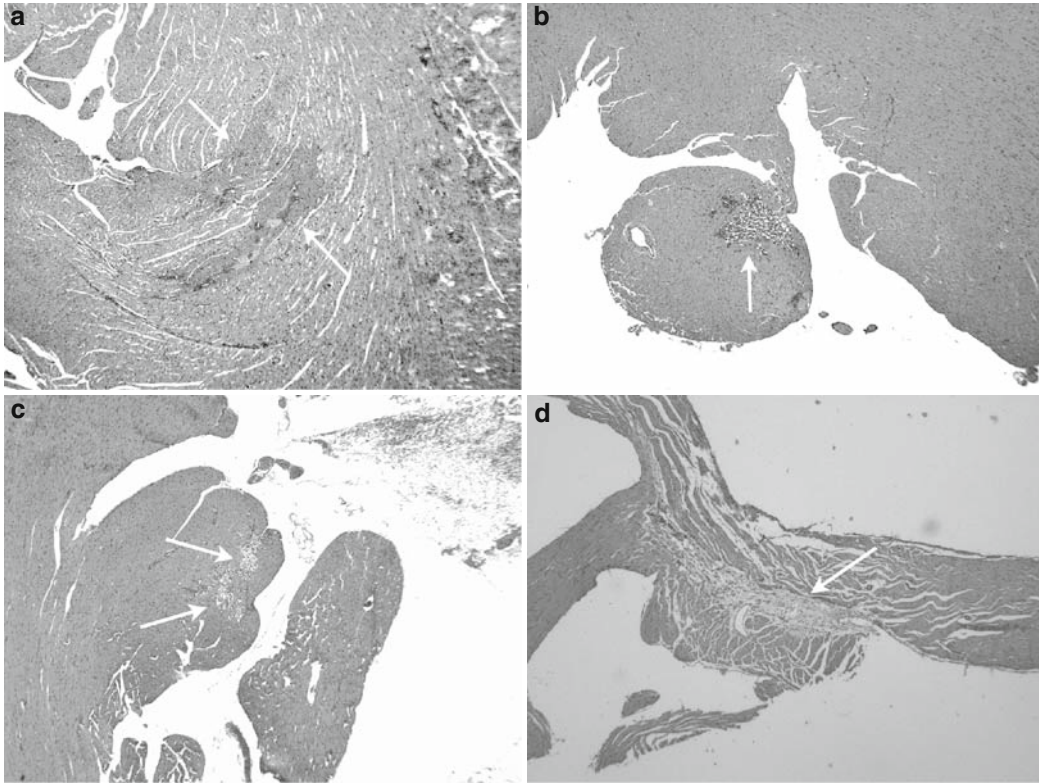


Fig. 2.1. Examples of myocardial ischemic lesions in JCR:LA-*cp* male rats (*cp/cp*) at 26 weeks of age. **Panel A:** Stage 1 lesion, area of necrosis without chronic inflammatory cell infiltration, in left ventricle. **Panel B:** Stage 2 lesion, area of active inflammatory cell activity and cell lysis, in lower trabecular muscle. **Panel C:** Stage 3 lesion, area of chronic inflammatory cell infiltration, without visible cell lysis, in trabecular muscle. **Panel D:** Stage 4, early scarred lesion with a small number of inflammatory cells or fibroblast, in upper perivalvular region of the heart. All images at $\times 20$, H&E stained sections, with lesions indicated by arrows.

15. Lesions detected by SEM are identified and classified as areas of adherent fibrin; raised intimal lesions; areas of adherent macrophages; or areas of de-endothelialization (53). The aortic arch, after fixation and processing, retains its *in vivo* morphology in two semi-rigid segments composed of compound curves. It is not possible either to flatten the arch or to obtain planar images of the arch and areas of lesion that are suitable for quantification through image analysis. Thus, images of all lesions are recorded and each type of lesion is assigned a “severity score,” based on area and character of the lesion. The scale ranges from 0 to 3, with 0 representing the absence of any lesions and 3 representing the most severe involvement, as seen in atherosclerotic control animals. The scores are summed for each animal.

Representative TEM images of atherosclerotic lesions in rats have been reported previously (54).

Acknowledgments

The advancement of Science builds on the contributions of those who went before us. The development of the laboratory rat can be traced to breeding and specialization of “fancy rats” in Kyoto, Japan dating to the seventeenth century (54). The modern experimental use of rats originated in The Wistar Institute in Philadelphia and from work of Henry Donaldson (55). Studies in our laboratory would not have been possible without the assistance of veterinarians David Secord and David Neil, senior technicians Dorothy Koeslag and Sandra Kelly, and many students and post-doctoral fellows. Essential financial support was provided by the Medical Research Council of Canada, the Heart and Stroke Foundation of Alberta and the Northwest Territories and a number of pharmaceutical firms.

References

1. Karsch, KR. (1992) Atherosclerosis – where are we heading? *Herz* **17**, 309–319.
2. Moore, S. (1981) Responses of the arterial wall to injury. *Diabetes* **30**(S 2), 8–13.
3. Ross, R. (1999) Atherosclerosis: an inflammatory disease. *N Engl J Med* **340**, 115–126.
4. Yusuf, S, Reddy, S, Ôunpuu, S, et al. (2001) Global burden of cardiovascular diseases Part I: general considerations, the epidemiological transition, risk factors, and impact of urbanization. *Circulation* **104**, 2746–2753.
5. Proctor, SD, Russell, JC. (2006) Small animal models of cardiovascular disease: tools for study of roles of the metabolic syndrome, dyslipidemias and atherosclerosis. *J Cardiovasc Pathol* **15**, 318–330.
6. Davignon, J, Genest, J. (1998) Genetics of lipoprotein disorders. *Endocrin Metab Clinics of N Amer* **27**, 521–550.
7. Brown, MS, Goldstein, JL. (1996) Heart attacks: gone with the century? *Science* **272**, 629.
8. Ornskov, F. (1998) In Jacotot, B, Mathé, D, Fruchart, J-C, (eds.), *Atherosclerosis XI: Proceedings of the 11th International Symposium on Atherosclerosis*. Elsevier Science, Singapore, pp. 925–32.
9. Hegele, RA, Zinman, B, Hanley, AJ, et al. (2003) Genes, environment and Oji-Cree type 2 diabetes. *Clin Biochem* **36**, 163–170.
10. Razak, F, Anand, S, Vuksan, V, Davis, B, et al. (2005) Ethnic differences in the relationships between obesity and glucose-metabolic abnormalities: a cross-sectional population-based study. *Int J Obesity* **29**, 656–667.
11. Richardson, M, Kurowska, EM, Carroll, KK. (1994) Early lesion development in the aortas of rabbits fed low-fat, cholesterol-free, semipurified diet. *Atherosclerosis* **107**, 165–178.
12. Richardson, M, Fletch, A, Delaney, K, et al. (1997) Increased expression of vascular cell adhesion molecule-1 by the aortic endothelium of rabbits with *Pasteurella multocida* pneumonia. *Lab Anim Sci* **47**, 27–35.
13. Bolzán, AD, Bianchi, MS. (2002) Genotoxicity of streptozotoc. *Mutat Res* **512**, 121–134.
14. Yang, Y, Santamaria, P. (2006) Lessons on autoimmune diabetes from animal models. *Clin Sci* **110**, 627–639.
15. Zucker, LM, Zucker, TF. (1961) Fatty, a new mutation in the rat. *J Hered* **52**, 275–278.
16. Chua, SC Jr, White, DW, Wu-Peng, XS, et al. (1996) Phenotype of fatty due to Gln269Pro mutation in the leptin receptor (Lepr). *Diabetes* **45**, 1141–1143.
17. Amy, RM, Dolphin, PJ, Pederson, RA, et al. (1988) Atherogenesis in two strains of obese rats: the fatty Zucker and LA/N-corpulent. *Atherosclerosis* **69**, 199–209.
18. Peterson, RG. (2001) The Zucker Diabetic Fatty (ZDF) rat. In Sima, AAF, Shafir, E,

- (eds.), *Animal Models of Diabetes a Primer*. Harwood Academic Publishers, Amsterdam, pp. 109–128.
19. Schäfer, S, Steiöff, K, Linz, W, et al. (2004) Chronic vasopeptidase inhibition normalizes diabetic endothelial dysfunction. *Euro J Pharmacol* **484**, 361–362.
 20. Oltman, CL, Richou, LL, Davidson, EP, et al. (2006) Progression of coronary and mesenteric vascular dysfunction in Zucker obese and Zucker Diabetic Fatty rats. *Am J Physiol Heart Circ Physiol* **291**, H1780–H1787.
 21. Marsh, SA, Powell, PC, Agarwal, A, et al. (2007) Cardiovascular dysfunction in Zucker obese and Zucker diabetic fatty rats: role of hydronephrosis. *Am J Physiol Heart Circ Physiol* **293**, H292–H298.
 22. Koletsky, S. (1975) Pathologic findings and laboratory data in a new strain of obese hypertensive rats. *Am J Pathol* **80**, 129–142.
 23. Wu-Peng, XS, Chua, SC Jr, Okada, N, et al. (1997) Phenotype of the obese Koletsky (*f*) rat due to Tyr763Stop mutation in the extracellular domain of the leptin receptor: evidence for deficient plasma-to-CSF transport of leptin in both the Zucker and Koletsky obese rat. *Diabetes* **46**, 513–518.
 24. Russell, JC, Graham, SE, Dolphin, PJ. (1999) Glucose tolerance and insulin resistance in the JCR:LA-cp rat: effect of miglitol (Bay m1099). *Metabolism* **48**, 701–706.
 25. Russell, JC, Bar-Tana, J, Shillabeer, G, et al. (1998) Development of insulin resistance in the JCR:LA-cp rat: role of triacylglycerols and effects of MEDICA 16. *Diabetes* **47**, 770–778.
 26. Vance, JE, Russell, JC. (1990) Hypersecretion of VLDL, but not HDL, by hepatocytes from the JCR:LA-corpulent rat. *J Lipid Res* **31**, 1491–1501.
 27. Russell, JC, Graham, SE, Richardson, M. (1998) Cardiovascular disease in the JCR:LA-cp rat. *Mol Cell Biochem* **188**, 113–126.
 28. O'Brien, SF, Russell, JC, Davidge, ST. (1999) Vascular wall dysfunction in JCR:LA-cp rats: effects of age and insulin resistance. *Am J Physiol* **277**, C987–C993.
 29. Proctor, SD, Kelly, SE, Russell, JC. (2005) A novel complex of arginine–silicate improves micro- and macrovascular function and inhibits glomerular sclerosis in insulin-resistant JCR:LA-cp rats. *Diabetologia* **48**, 1925–1932.
 30. Richardson, M, Schmidt, AM, Graham, SE, et al. (1998) Vasculopathy and insulin resistance in the JCR:LA-cp rat. *Atherosclerosis* **138**, 135–146.
 31. McCune, S, Park, S, Radin, MJ, et al. (1995) The SHHF/Mcc-facp: a genetic model of congestive heart failure. In Singal, PK, Beamish, RE, Dhalla, NS, (eds.), *Mechanisms of Heart Failure*. Kluwer Academic, Boston, MA, pp. 91–106.
 32. Janssen, PML, Stull, LB, Leppo, MK, et al. (2002) Selective contractile dysfunction of left, not right, ventricular myocardium in the SHHF rat. *Am J Physiol Heart Circ Physiol* **284**, H772–H778.
 33. Emter, CA, McCune, SA, Sparagna, GC, et al. (2005) Low-intensity exercise training delays onset of decompensated heart failure in spontaneously hypertensive heart failure rats. *Am J Physiol Heart Circ Physiol* **289**, H2030–H2038.
 34. Portha, B. (2005) Programmed disorders of β -cell development and function as one cause for type 2 diabetes? The GK rat paradigm. *Diabetes Metab Res Rev* **21**, 495–504.
 35. Matsumoto, T, Kakami, M, Noguchi, E, et al. (2007) Imbalance between endothelium-derived relaxing and contracting factors in mesenteric arteries from aged OLETF rats, a model of Type 2 diabetes. *Am J Physiol Heart Circ Physiol* **293**, H1480–H1490.
 36. Kagota, S, Tanaka, N, Kubota, Y, et al. (2004) Characteristics of vasorelaxation responses in a rat model of metabolic syndrome. *Clin Exp Pharmacol Physiol* **31**, S54–S56.
 37. Vine, D, Takechi, R, Russell, JC, et al. (2007) Impaired postprandial apolipoprotein-B48 metabolism in the obese, insulin-resistant JCR:LA-cp rat: increased atherogenicity for the metabolic syndrome. *Atherosclerosis* **190**, 282–290.
 38. Mangat, R, Su, J, Scott, PG, Russell, et al. (2007) Chylomicron and apoB48 metabolism in the JCR:LA corpulent rat, a model for the metabolic syndrome. *Biochem Soc Trans* **35**, 477–481.
 39. Pooley, SM. (1960) A systematic method of breeder rotation for non-inbred laboratory animal colonies. *Animal Care Panel* **10**, 159–161.
 40. Russell, JC, Koeslag, DG, Amy, RM, et al. (1989) Plasma lipid secretion and clearance in the hyperlipidemic JCR:LA-corpulent rat. *Arteriosclerosis* **9**, 869–876.
 41. Radomski, MW, Salas, E. (1995) Nitric oxide-biological mediator, modulator and factor of

- injury: its role in the pathogenesis of atherosclerosis. *Atherosclerosis* **118**, S69–S80.
42. De Lean, A, Munson, PJ, Rodbard, D. (1978) Simultaneous analysis of families of sigmoidal curves: application to bioassay, radioligand assay, and physiological dose-response curves. *Am J Physiol* **235**:E97–E102.
 43. Leza, JC, Salas, E, Sawicki, G, et al. (1998) The effect of stress on homeostasis in JCR:LA-cp rats. Role of nitric oxide. *J Pharmacol Exp Ther* **28**, 1397–1403.
 44. Russell, JC, Proctor, SD, Kelly, SE, Brindley, DN. (2008) Pair feeding-mediated changes in metabolism: stress response and pathophysiology in insulin resistant, atherosclerosis-prone JCR:LA-cp rats. *Am J Physiol Endocrinol Metab*, **294**, E1078–1087.
 45. Russell, JC, Ravel, D, Pégrier, J-P, et al. (2000) Beneficial insulin-sensitizing and vascular effects of S15261 in the insulin-resistant JCR:LA-cp rat. *J Pharmacol Exp Ther* **295**, 753–760.
 46. Hanusch, C, Hoeger, S, Beck, GC. (2007) Anaesthesia of small rodents during magnetic resonance imaging. *Methods* **43**, 68–78.
 47. Russell, JC, Amy, RM, Manickavel, V, et al. (1987) Insulin resistance and impaired glucose tolerance in the atherosclerosis prone LA/N-corpulent rat. *Arteriosclerosis* **7**, 620–626.
 48. Russell, JC, Graham, S, Hameed, M. (1994) Abnormal insulin and glucose metabolism in the JCR:LA-corpulent rat. *Metabolism* **43**, 538–543.
 49. Russell, JC, Dolphin, PJ, Graham, SE, et al. (1998) Improvement of insulin sensitivity and cardiovascular outcomes in the JCR:LA-cp rat by d-fenfluramine. *Diabetologia* **41**, 380–389.
 50. Russell, JC, Bar-Tana, J, Shillabeer, G, et al. (1998) Development of insulin resistance in the JCR:LA-cp rat: role of triacylglycerols and effects of MEDICA 16. *Diabetes* **47**, 770–778.
 51. Russell, JC, Amy, RM, Graham, S, et al. (1993) Effect of castration on hyperlipidemic, insulin resistant JCR:LA-corpulent rats. *Atherosclerosis* **100**, 113–122.
 52. Ferrario, F, Rastaldi MP. (2006) Histopathological atlas of renal diseases: diabetic nephropathy. *J Nephrol* **19**, 1–5.
 53. Russell, JC, Amy, RM, Graham, SE, et al. (1995) Inhibition of atherosclerosis and myocardial lesions in the JCR:LA-cp rat by β,β' -tetramethylhexadecanedioic acid (MEDICA 16). *Arterioscler Thromb Vasc Biol* **15**, 918–923.
 54. Mashimo, T, Voigt, B, Kuramoto, T, et al. (2005) Rat phenotype project: the untapped potential of existing rat strains. *J Appl Physiol* **98**, 371–379.
 55. Lindsay, JR. (1976) Historical Foundations. In Baker, HJ, Lindsay, JR, Weisbroth, SH (eds.), *The Laboratory Rat*. Academic Press, Orlando, pp. 1–36.



<http://www.springer.com/978-1-60761-246-9>

Cardiovascular Genomics

Methods and Protocols

DiPetrillo, K. (Ed.)

2009, X, 350 p. 84 illus., Hardcover

ISBN: 978-1-60761-246-9

A product of Humana Press